IJASRM
International Journal of Advanced Scientific Research and Management, Vol. 2 Issue 8, August 2017.
www.ijasrm.com
ISSN 2455-6378

Preparation, Characterization and Biological Activity Evaluation of some Metal Complexes from Novel Schiff Bases based on Ambroxol Drug

Walaa H. Mahmoud [1], Mostafa M.H Khalil [2], Hoda A. Elsawy [3], Gehad G. Mohamed [1], Mostafa A. Radwan [3]

[1] Chemistry Department, Faculty of Science, Cairo University, Giza, 12613, Egypt

[2] Chemistry Department, Faculty of Science, Ain Shams University, Cairo, Egypt

[3] Chemical Engineering Department, Faculty of Engineering, British University in Egypt, Cairo, Egypt

Abstract

Novel Schiff bases were prepared as the condensation product of reaction of 2-hydroxybenzaldehyde and ambroxol drug (H_2L^1) and the second one from the reaction of 2-quinoline carbaldehyde with ambroxol (HL^2). The synthesized Schiff basses were acted as a tridentate ligand for the preparation of new complexes through reaction with the metal ions of Cd(II) and Sn(II). The newly prepared Schiff bases and their metal complexes were characterized using some physicochemical techniques including elemental analysis, FT-IR, UV–Vis, mass spectrometry, conducti-metric measurements as well as thermal analyses (TGA/DTG),. On the basis of these studies, an octahedral geometry for both Cd(II) and Sn(II) complexes has been suggested. The antimicrobial activity against some species of bacteria and fungi organisms was employed to the two Schiff bases and their complexes. The results showed that the Cd(II) complex recorded the highest antimicrobial activity.

Key words *Schiff base, Ambroxol, UV–Vis, FT-IR, Thermal analyses and Antimicrobial activity.*

1. Introduction

Schiff bases can be synthetized when any primary amine reacts with a ketone or an aldehyde under particular circumstances. Schiff base (also identified as azomethine) is a nitrogen analogue of the used aldehyde or ketone where the carbonyl group (CO) has been substituted by azomethine (imine) group [1].

Schiff bases and their derivatives have been described to plays an important role concerning the biological activities such as antibacterial, antifungal, antiviral, antimalarial, anti-inflammatory and antipyretic properties which is encountering for the azomethine group present in such compounds [2]. They also can act as catalytic agents as well as having a role in Dye and polymer formation [3].

Ambroxol is acts as an antioxidant, anti-inflammatory, mucolytic agent and helps in blocking of Na^+ ion channel. It can motivate surfactant secretion and produces expectorant effects by decreasing mucus linkage to the bronchial of the lining. It limits histamine secretion from the mast cells. Ambroxol is a muco-active

substance in which can be used for the management of acute and chronic bronchitis [4].

In the presented study, a two novel Schiff base ligands were synthesized by condensation of 2-hydroxybenzaldehyde and 2-quinoline carbaldehyde with ambroxol drug. Their mode of complexation with Cd(II) and Sn(II) metal ions was examined. Also their antimicrobial activity was demonstrated.

2. Experimental

2.1 Materials and reagents:

All the chemicals used were of the analytical reagent grade (AR), and of highest purity available. They included 2-hydroxybenzaldehyde, 2-quinoline carbaldehyde, ambroxol, $CdCl_2$ and $SnCl_2$ which were provided from Aldrich, Aldrich, Nile Pharma, Sigma and Aldrich, respectively.

Organic solvent used was ethyl alcohol (99 and 95%). De-ionized water was usually used in all preparations.

2.2 Solution

Fresh stock solutions of ($1x10^{-3}$ M) H_2L^1 and HL^2 ligands were prepared by dissolving the appropriate weight amount of them (0.4 g/L) in the suitable volume of ethyl alcohol. Solutions of the Schiff base ligands and its metal complexes ($1x10^{-4}$ M and $1x10^{-5}$ M) were prepared by dilution of the previous prepared stock solutions for measuring their UV-Vis spectra.

2.3 Instruments

Mass spectra were recorded by the EI technique at 70 eV using MS-5988 GS-MS Hewlett–Packard instrument at the Microanalytical Center, National Center for Research, Egypt. Molar conductivities of 10^{-3} M solutions of the solid complexes in ethanol were measured using Jenway 4010 conductivity meter. The molar magnetic susceptibility was measured on powdered samples using the Faraday method. The diamagnetic corrections were made by Pascal's constant and $Hg[Co(SCN)_4]$ was used as a calibrant.. Microanalyses of carbon, hydrogen and nitrogen were carried out at the Microanalytical Center, Cairo University, Egypt, using CHNS-932 (LECO) Vario Elemental Analyzer. Analyses of the metals followed the dissolution of the solid complexes in concentrated HNO_3, neutralizing the diluted aqueous solutions with ammonia and titrating the metal solutions with EDTA. FT-IR spectra were recorded on a Perkin-Elmer 1650 spectrometer (4000–400 cm^{-1}) in KBr pellets. Electronic spectra were recorded at room temperature on a Shimadzu 3101pc spectrophotometer as solutions in ethanol.^{1}H NMR spectra, as a solution in DMSO-d_6, were recorded on a 300 MHz Varian-Oxford Mercury at room temperature using TMS as an internal standard. UV-Vis spectra were carried out on UV mini-1240, UV-Vis spectrophotometer, Shimadzu. The thermogravimetric analyses (TG and DTG) of the solid complexes were carried out from room temperature to 1000 ºC using a Shimadzu TG-50H thermal analyzer. The antimicrobial activities were carried out at the Microanalytical Center, Cairo University, Egypt.

2.4 Synthesis of Schiff base (H_2L^1 and HL^2) ligands

The Schiff base ligands (H_2L^1 and HL^2) were synthetized by refluxing a mixture of 2-hydroxybenzaldehyde (6.61 mmol, 0.69 mL) and 2-quinoline carbaldehyde (6.61 mmol, 1.04 g) with ambroxol (6.61 mmol, 2.5 g), respectively, dissolved in ethanol. The resulting mixture was stirred under reflux for about 2 hours at temperature (100-150 ºC) during which a brown and reddish brown solid compounds were separated. They were filtered, recrystallized and washed with DMF and dried in vacuum.

2.5 Synthesis of the metal chelates

The metal complexes were prepared by the addition of hot solution (60 ºC) of the appropriate metal chloride (0.83 mmol) and (0.77mmol) in an ethanol (25 mL) to the hot solution (60 ºC) of the H_2L^1 (0.4 g/L, 0.83 mmol) and HL^2 (0.4 g/L, 0.77 mmol) ligands in ethanol (25 mL), respectively. The formed mixture was stirred under reflux for two hours where upon the complexes precipitated. They were obtained by filtration, washed with a little amount of hot DMF and dried in vacuum desiccator over anhydrous calcium chloride. The analytical data for C, H and N were repeated twice.

3. Pharmacology

3.1 Antimicrobial activity

A filter paper disk (5 mm) was transferred into 250 ml flasks containing 20 mL of working volume of tested solution (100 mg/mL). All flasks were autoclaved for 20 min at 121 ºC. LB agar media surfaces were inoculated with four investigated bacteria (Gram positive bacteria: *Bacillus Subtilis* and *Streptococcus pneumoniae*; Gram negative bacteria*: Salmonella SP*. And *Escherichia coli*) and fungi (*Aspergillus fumigatus*

and *Candida albicans*) by diffusion agar technique [5,6,7] then, transferred to a saturated disk with a tested solution in the center of Petri dish (agar plates). All the compounds were placed at 4 equidistant places at a distance of 2 cm from the center in the inoculated Petriplates. DMSO served as control. Finally, all these Petri dishes were incubated at 25 ºC for 48 h where clear or inhibition zones were detected around each disk. Control flask of the experiment was designed to perform under the same condition described previously for each microorganism but with dimethylformamide solution only and by subtracting the diameter of inhibition zone resulting with dimethylformamide from that obtained in each case, so antibacterial activity could be calculated [8,9]. Amikacin and ketokonazole were used as reference compounds for antibacterial and antifungal activities, respectively. All experiments were performed as triplicate and data plotted were the mean value.

4. Results and discussion

4.1 Characterization of the Schiff base ligands

The brown Schiff base ligand (H_2L^1) and the reddish brown Schiff base ligand (HL^2) were prepared by the self-condensation reaction of 2-hydroxybenzaldehyde and 2-quinoline carbaldehyde with ambroxol drug, respectively, using ethanol as a solvent, the formed Schiff base ligands were steady in air and soluble in various organic solvents. The data obtained from the elemental analysis of C, H and N content of H_2L^1 and HL^2 referred to ($C_{20}H_{22}Br_2N_2O_2$) and ($C_{23}H_{23}Br_2N_3O$) were shown as C, 49.34 and 55.21; H, 4.16 and 3.34; N, 5.72 and 8.02, calculated: C, 49.79 and 55.38; H, 4.56 and 4.45; N, 5.81 and 8.13, respectively, there was good agreement between both of the experimental and theoretical data which prove the proposed formula.

Preparation of H_2L^1 and HL^2 ligands were confirmed by the appearance of a strong IR band at 1619 and 1630 cm^{-1}, respectively, resulting from the formation of azomethine (ν(C=N)) group, while the bands attributable to ν(NH_2) or ν(C=O) of the forming aldehydes and the ambroxol drug have not been observed [10]. The ν(OH) stretching band was observed at 3413 and 3422 cm^{-1}, respectively, on the other hand, the ν(NH) bending band was appeared at 640 and 618 cm^{-1}, respectively, as its stretching band was overlapped with the OH band.

The proton ^1H NMR spectrum was recorded for H_2L^1 ligand in which the phenolic group has been appeared as singlet at 10.26 ppm while the aromatic protons have been appeared as a set of multiplet in the region 6.94 –7.62 ppm and the NH proton appeared as multiplet at the region 3.37 – 3.45 ppm. While in the case of the HL^2 ligand, the aliphatic OH proton appeared as singlet signal at 4.90 ppm, the aromatic protons showed multiplet signal at the region of 7.50 – 8.65 ppm and the NH proton appeared as singlet signal at 4.09 ppm.

The mass spectrum of H_2L^1 and HL^2 ligands exhibit a molecular ion peak at m/z = 485.62 and 516.85 amu corresponding to [M+3] and [M], respectively, which confirmed the proposed formula $[C_{20}H_{22}Br_2N_2O_2]^{\cdot+}$ and $[C_{23}H_{23}Br_2N_3O]^{\cdot+}$ with atomic mass of 482 and 517 amu, respectively. The structure of the proposed Schiff base ligands was illustrated in Figure (1).

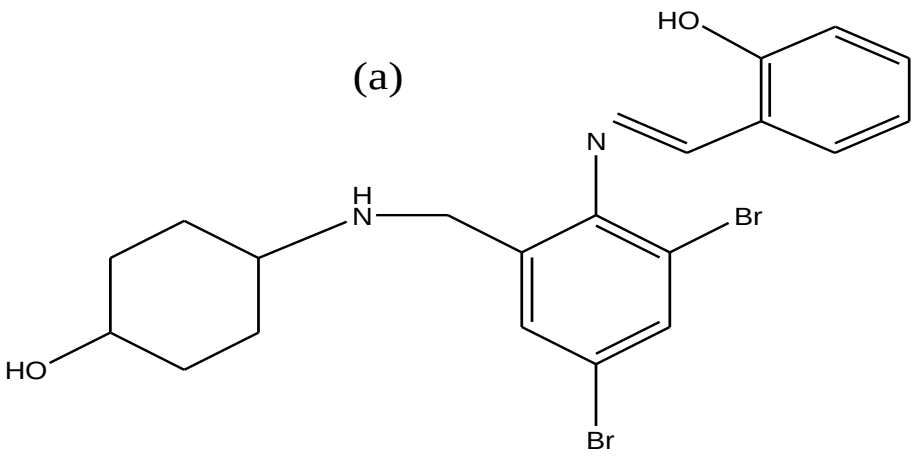

IJASRM
International Journal of Advanced Scientific Research and Management, Vol. 2 Issue 8, August 2017.
www.ijasrm.com
ISSN 2455-6378

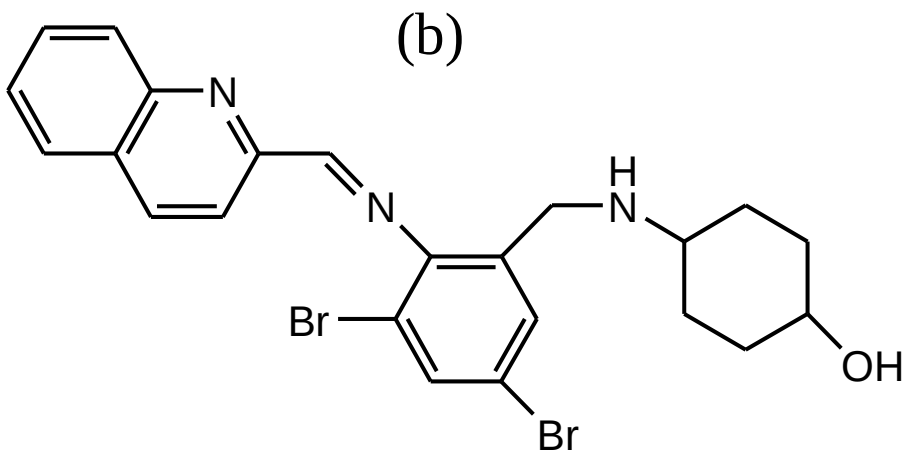

Figure 1. Structures of (a) H_2L^1 and (b) HL^2 ligands.

4.2 Characterization of metal complexes

All of the formed complexes were having a colour and stable to air. They were soluble in many organic solvents including ethanol. The complexes were characterized by different techniques such as elemental analyses, ^{1}H NMR, IR spectral, mass and thermal analysis. The structure of the formed complexes were demonstrated in Figure (2, 3).

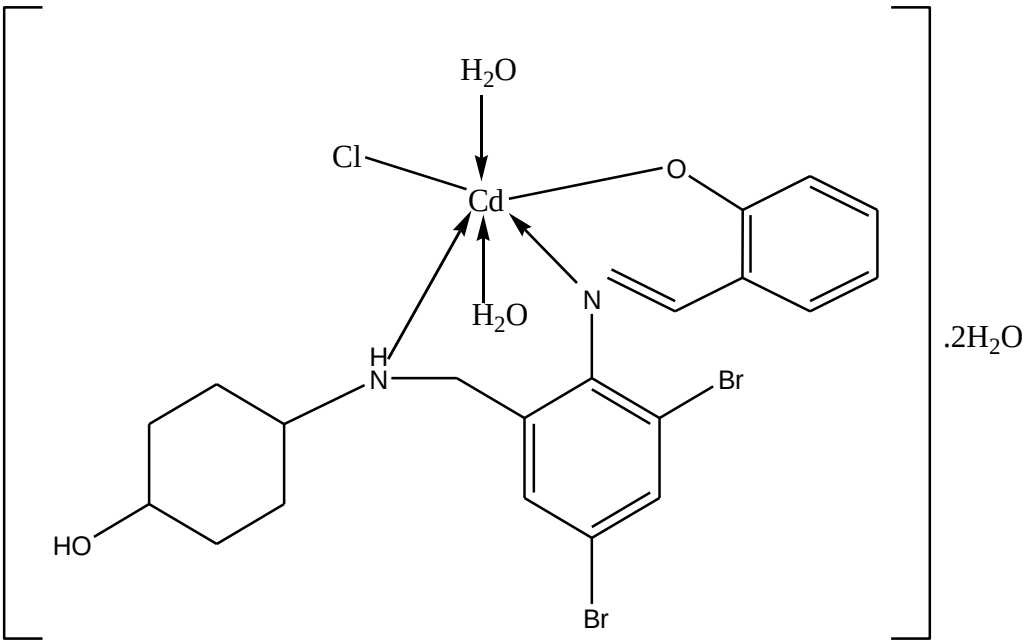

Compound (Molecular Formula)	Colour (% yield)	M.P. (^oC)	% Found (Calcd)					Λ_m $\Omega^{-1}mol^{-1}cm^2$
			C	H	N	Cl	M	

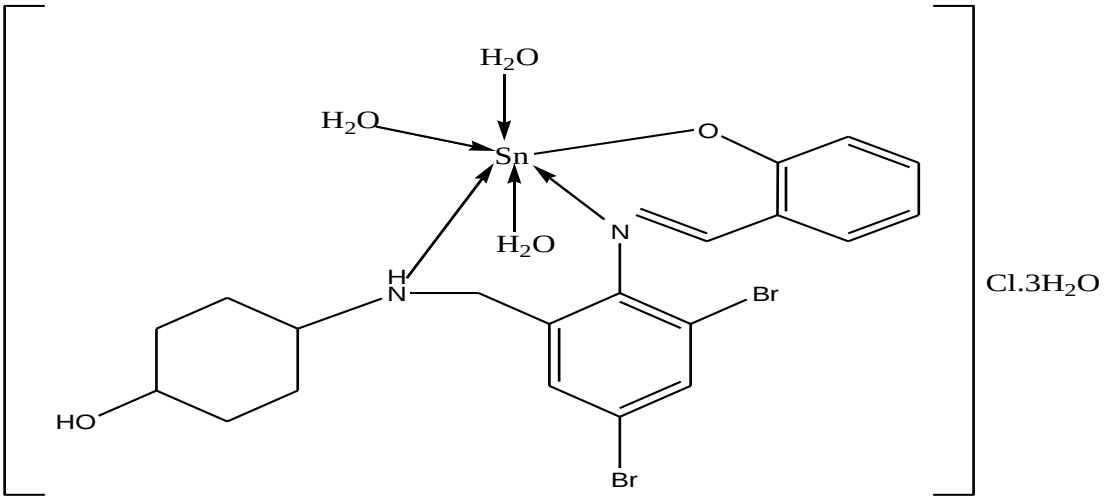

Figure 2. Structures of metal complexes of H_2L^1 ligand.

4.3 Elemental analysis

Both experimental and theoretical results of the elemental analysis of the synthetized complexes have a high degree of accordance to each other which point out that the metal complexes of Schiff base ligands were formed in 1:1 ratio and they had the composition of MHL type. The results of elemental analyses of Cd(II) and Sn(II) metal complexes (C, H, N, Cl and M) and melting point were scheduled in Table (1)

.

Table (1). Analytical and physical data of the two Schiff bases and their Cd(II) and Sn(II) metal complexes.

(H_2L^1) $C_{20}H_{22}Br_2N_2O_2$	Brown (90)	132	49.34 (49.79)	4.16 (4.56)	5.72 (5.81)	-----	-----	
$[Cd(HL^1)(H_2O)_2Cl].2H_2O$	Gray (87)	160	34.15 (34.24)	4.08 (4.14)	3.81 (3.99)	5.00 (5.06)	15.76 (15.98)	34
$[Sn(HL^1)(H_2O)_3]Cl.3H_2O$	Brown (83)	152	32.13 (32.30)	4.00 (4.44)	3.65 (3.77)	4.62 (4.78)	15.72 (15.97)	90
(HL^2) $C_{23}H_{23}Br_2N_3O$	Reddish brown (92)	140	55.21 (53.38)	4.34 (4.45)	8.02 (8.13)	-----	-----	
$[Cd(HL^2)(H_2O)Cl_2].2H_2O$	Brown (86)	165	36.25 (36.60)	3.59 (3.85)	5.16 (5.57)	9.26 (9.42)	14.46 (14.85)	46
$[Sn(HL^2)(H_2O)_3].Cl_2$	Reddish brown (82)	168	36.11 (36.28)	3.54 (3.81)	9.06 (9.12)	9.14 (9.33)	15.36 (15.60)	113

4.4 Infrared spectra and mode of bonding

The infrared spectral data for the Schiff base ligands and their metal complexes are enumerated in Table (2). The free H_2L^1 and HL^2 ligands FT-IR spectra were matched with that of the formed complexes in order to allocate the coordination sites resulting in the chelation process. The FT-IR spectra of the metal complexes showed a broad band around 3420–3426 cm^{-1} which may be assigned to ν(OH), while it appears in the H_2L^1 and HL^2 ligands spectra at 3413 and 3422 cm^{-1}, respectively. The ligands FT-IR spectra spectacle a distinguishable absorption band at 1619 and 1630 cm^{-1}, that may be attributed to ν(C=N) of azomethine group; on the other hand, this band was shifted to a higher or lower wavelength in the metal complexes and it appeared at the range 1615-1629 cm^{-1}. It was perceived that the ν(NH) bending band was appeared at 640 and 618 cm^{-1} for H_2L^1 and HL^2 ligands, respectively, while in the Cd(II) and Sn(II) metal complexes, it was shifted to appear in the range of 616-660 cm^{-1} as per that the stretching band of ν(NH) wasn't be able to described because of its intersecting with ν(OH) stretching band. The coordinating water molecules in the complexes are characterized by the occurrence of two bands at 863–955 and 755–870 cm^{-1} [11]. The synchronization of the nitrogen of the azomethine (imine) group is established by the presence of a new metal–ligand weak band at 410–445 cm^{-1} due to ν(M-N) [12]. Another new weak band at 541-588 cm^{-1} has appeared which might be attributed to the formation of M-O bond in the metal complexes [13]. It was concluded from the previous data that the prepared H_2L^1 ligand acts as a mono-negative tridentate ligand that binds to the metal ion through two nitrogen atoms (azomethine nitrogen and ambroxol nitrogen) and one oxygen atom while HL^2 ligand acts as a neutral tridentate ligand that binds to the metal ion through three nitrogen atoms (azomethine nitrogen, ambroxol nitrogen and the pyridine nitrogen).

Table (2). IR spectra (4000-400 cm^{-1}) of H_2L^1, HL^2 ligand and their Cd(II) and Sn(II) metal complexes.

(H_2L^1)	$[Cd(HL^1)(H_2O)_2Cl].2H_2O$	$[Sn(HL^1)(H_2O)_3]Cl.3H_2O$	HL^2	$[Cd(HL^2)(H_2O)Cl_2].2H_2O$	$[Sn(HL^2)(H_2O)_3].Cl_2$	Assignment
3413br	3420br	3426br	3422br	3425br	3424br	OH
1619sh	1627sh	1615sh	1630sh	1629sh	1627sh	C=N
-----	-----	-----	1074m	1072sh	1068sh	Pyridine ring stretching
----- -----	871m, 755m	955s 870m	----- -----	864s 768s	863s 765s	H_2O stretching of coordinated water

640w	656w	660w	618s	616m	620w	NH bending
-----	588m	541s	-----	530w	547w	M-O
-----	445w	445w	-----	410w	420w	M-N

sh = sharp, m = medium, br = broad, s = small, w = weak

4.5 ^{1}H NMR spectral studies of the metal complexes

Upon matching the proton signals position in the Cd(II) complexes with those of the free ligands, it can be detected that all signals were in the expected region but only showed a slight shift due to the coordination of the ligand to the metal ion[14]. The multiplet signals in the region 6.94-7.62 and 7.50–8.65 ppm in H_2L^1 and HL^2 ligands, respectively, may be attributed to aromatic protons [14,15], on the other hand, they appeared at 6.92–7.64 and 7.42– 8.22ppm in $[Cd(HL^1)(H_2O)_2Cl].2H_2O$ and $[Cd(HL^2)(H_2O)Cl_2].2H_2O$ complexes, respectively. The singlet signal observed at 10.26 ppm in the ^{1}H NMR spectrum of H_2L^1 ligand, which may be corresponded to the phenolic proton, has disappeared in the spectrum of formed Cd(II) complex. The multiplet signals in the region 3.37-3.45 ppm in the Schiff base ligands which may be attributed to NH group, was shifted to appear at 3.37-3.57 and 4.11 ppm in $[Cd(HL)(H_2O)_2Cl].2H_2O$ and $[Cd(HL^2)(H_2O)Cl_2].2H_2O$ complexes, respectively. On the other hand, the singlet signal that was appeared at 4.12 and 4.90 in the free ligands which can be assigned to the aliphatic, have't been changed in the metal complexes which proves that it had not any cooperation role in the metal complex formation. From ^{1}H NMR data it was conclouded from the deporotonation of the phenolic group in H_2L^1 ligand and proved the formation of complex by binding of metal ions to the oxygen atom of phenol group and the participation of NH group in the complexation process og the two ligands to the Cd(II) metal ion.

4.6 Molar conductance measurements

The solubility of the complexes in ethanol allowed the determination of the molar conductivity (Λ_m) of 10^{-3} M solutions for all complexes at 25ºC. It was concluded from the results that $[Cd(HL^1)(H_2O)_2Cl].2H_2O$ and $[Cd(HL^2)(H_2O)Cl_2].2H_2O$ complexes had molar conductance values of 34 and 46 Ω^{-1} mol^{-1} cm^2, respectively, indicating their weak ionic nature (non-electrolytes). This confirmed that the anions were involved in the coordination sphere [16]. On the other hand, $[Sn(HL^1)(H_2O)_3]Cl.3H_2O$ complex had molar conductance value of 90 Ω^{-1} mol^{-1} cm^2 indicated its ionic nature and that it was of the type 1:1 electrolyte, while $[Sn(HL^2)(H_2O)_3].Cl_2$ complex showed molar conductance value of 113 Ω^{-1} mol^{-1} cm^2 indicating its ionic nature and that it was 1:2 electrolyte. The molar conductance data was demonstrated in Table (1).

4.7 Thermal analysis studies (TGA and DTG)

The thermogravimetric technique (TG) and differential thermogravimetric (DTG) analyses for the H_2L^1 and HL^2 ligands and its metal complexes were explained in Table (3) within the temperature range from 50 to 1000 ºC.

The TG data for H_2L^1 Schiff base ligand showed three decomposition platforms. The first stage within the temperature range of 50-245 ºC and a maximum temperature of 115 ºC, which resembles to the evaluation of C_2H_4N molecule with mass loss of 8.40 % (calculated mass loss = 8.67 %). The second decomposition step was found within the temperature range of 245-475 ºC and a maximum temperature of 360 ºC, which corresponds to the loss of C_8H_8N molecule with mass loss of 24.23 % (calculated mass loss = 24.50 %).The final decomposition stage in the temperature range of 475-1000 ºC correspond to complete decomposition of the remaining part of the ligand ($C_{10}H_{10}Br_2O_2$) with mass loss of 68.92 % (calculated mass loss = 66.75 %). The DTG curve provided maximum peak temperature at 645 ºC and the total weight loss amounted to 98.60 % (calcd. 99.90 %).

The thermogravimetric (TG) curve for $[Cd(HL^1)(H_2O)_2Cl].2H_2O$ complex displayed four weight loss steps in the temperature range of 50-1000 ºC. The first stage of decomposition arisen within the range of 50-170 ºC, with a temperature maximum at 105 ºC which related to the loss of the two water molecules of hydration, with estimated mass loss of 5.96 % (calculated mass loss = 5.14 %). The next step of decomposition was detected within the range of 170-400 ºC, with a temperature maximum at 270 ºC that may be attributed to the loss of the two molecules of coordinated water along with $C_5H_{11}ClN$ fragment, where the mass loss was found to be 21.86 % (calculated mass loss = 22.33 %). The third stage of decomposition was observed within the range of 400-620 ºC, with a temperature maximum at 550 ºC and corresponds

to the loss of a C_5H_8Br molecule with an estimated mass loss of 21.44 % (calculated mass loss = 21.11 %). The remained fragment decomposed in the temperature range of 620-1000 ºC with a temperature maximum at 810 ºC that may be corresponded to the loss of a $C_{10}H_2BrNO$ fragment, with an estimated mass loss of 32.5 7% (calculated mass loss = 33.10 %) leaving CdO metal oxide as a residue. The overall weight loss was evaluated as 81.90 % (calculated mass loss = 81.68 %).

The thermogram for $[Sn(HL^1)(H_2O)_3]Cl.3H_2O$ complex showed four stages of decomposition. The first two stages within the temperature range of 50-320 ºC with a temperature maxima of 115 and 285 ºC, which may be related to the loss six molecules of water along with C_5H_6Cl fragment with mass loss of 29.42 % (calculated mass loss = 28.20 %). The third decomposition step was observed within the temperature range of 320-630 ºC and a temperature maximum of 360 ºC, which may be attributed to the loss of $C_6H_5Br_2$ molecule with mass loss of 31.57 % (calculated mass loss = 31.89 %). The final decomposition step in the temperature range of 630-1000 ºC corresponded to complete decomposition of the remaining part of the ligand ($C_9H_{10}N_2O$) with mass loss of 21.16 % (calculated mass loss = 21.80 %). The DTG curve gave maximum peak temperature at 865 ºC and the total weight loss amounted to 81.24% (calcd. 81.87 %) and SnO metal oxide was remained as a residue.

The TG data for HL^2 Schiff base ligand showed four stages of decomposition. The first two stages within the temperature range of 50-300 ºC with a temperature maxima of 90 and 225 ºC, which corresponded to the evaluation of $C_8H_{10}NO$ molecule with mass loss of 26.01 % (calculated mass loss = 26.30 %). The third decomposition step was found within the temperature range of 300-605 ºC and a temperature maximum of 450 ºC, which corresponds to the loss of $C_5H_6Br_2$ molecule with mass loss of 43.24 % (calculated mass loss = 43.71 %). The final decomposition stage in the temperature range of 605-1000 ºC may be related to complete decomposition of the remaining part of the ligand ($C_{10}H_7N_2$) with mass loss of 30.26 % (calculated mass loss = 30.04 %). The DTG curve gave maximum peak temperature at 730 ºC and the total weight loss amounted to 99.50 % (calcd. 99.90 %).

The thermogravimetric (TG) curve for $[Cd(HL^2)(H_2O)Cl_2].2H_2O$ complex exhibited five weight loss steps in the temperature range of 50-940 ºC. The first step of decomposition occurred within the range of 50-150 ºC, with a temperature maximum at 95 ºC which corresponds to the loss of the two water molecules of hydration, with estimated mass loss of 4.10 % (calculated mass loss = 4.77 %). The next step of decomposition was observed within the range of 150-380 ºC, with a temperature maximum at 305 ºC that may be related to the loss of the one molecule of coordinated water along with $C_3H_7Cl_2N$ fragment, where the mass loss was found to be 19.92 % (calculated mass loss = 19.36 %). The third stage of decomposition was observed within the range of 380-560 ºC, with a temperature maximum at 465 ºC and corresponds to the loss of a $C_8H_8Br_2$ molecule with an estimated mass loss of 34.48 % (calculated mass loss = 35.01 %). The remained fragment decomposed in the temperature range of 560-940 ºC with a two maxima at 630 and 670 ºC that may be related to the loss of a $C_{12}H_{10}N_2O$ fragment, with an estimated mass loss of 29.08 % (calculated mass loss = 28.38 %) leaving CdO metal oxide as a residue. The overall weight loss was evaluated as 87.76 % (calculated mass loss = 87.52 %).

The thermogravimetric (TG) curve for $[Sn(HL^2)(H_2O)_3].Cl_2$ complex showed a weight loss pattern over four stages. The first step of decomposition was observed within the range of 50-330 ºC, with a temperature maximum at 115 ºC that may be attributed to the loss of the three molecules of the coordinated water and the organic fragment $C_2H_8Cl_2N$ with estimated mass loss of 22.23 % (calculated mass loss = 22.54 %). The second step of decomposition was observed within the range of 330-625 ºC, with a temperature maximum at 420 ºC, related to the loss of a C_5H_5BrN fragment which having an estimated mass loss of 20.68 % (calculated mass loss = 20.92 %). The third and fourth steps of decomposition arisen in the range of 625-1000 ºC with two maxima at 825 and 865 ºC and may be correspond to the loss of $C_{16}H_{10}BrN$ fragment with estimated mass loss of 39.56 % (calculated mass loss = 38.91 %) leaving SnO oxide as a residue. The overall weight loss was evaluated as 82.47 % (calculated mass loss = 82.37%).

IJASRM International Journal of Advanced Scientific Research and Management, Vol. 2 Issue 8, August 2017.
www.ijasrm.com
ISSN 2455-6378

Table (3). Thermoanalytical results (TG and DTG) of H_2L^1, HL^2 ligand and their Cd(II) and Sn(II) metal complexes.

Complex	TG range (°C)	DTGmax (°C)	n*	Mass loss Estim (Calcd) %	Total mass loss	Assignment	Metallic residue
(H_2L^1)	50 – 245 245 – 475 475 - 1000	115 360 645	1 1 1	8.40 (8.67) 24.23 (24.50) 68.92 (66.75)	98.60 (99.90)	Loss of C_2H_4N. Loss of C_8H_8N. Loss of $C_{10}H_{10}Br_2O_2$.	---------
$[Cd(HL^1)(H_2O)_2Cl].2H_2O$	50 - 170 170 - 400 400 – 620 620 - 1000	105 270 550 810	1 1 1 1	5.96 (5.14) 21.86 (22.33) 21.44 (21.11) 32.57 (33.10)	81.90 (81.68)	Loss of $2H_2O$. Loss of $2H_2O$ and $C_5H_{11}ClN$. Loss of C_5H_8Br. Loss of $C_{10}H_2BrNO$.	CdO
$[Sn(HL^1)(H_2O)_3]Cl.3H_2O$	50- 320 320 - 630 630 – 1000	115, 285 360 865	2 1 1	28.42 (28.20) 31.57 (31.89) 21.16 (21.80)	81.24 (81.87)	Loss of $6H_2O$ and C_5H_6Cl. Loss of $C_6H_5Br_2$. Loss of $C_9H_{10}N_2O$.	SnO
(HL^2)	50 – 300 300 – 605 605 - 1000	90, 225 450 730	2 1 1	25.01 (26.30) 44.24 (43.71) 30.26 (30.04)	99.5 (99.9)	Loss of $C_8H_{10}NO$. Loss of $C_5H_6Br_2$. Loss of $C_{10}H_7N_2$.	---------
$[Cd(HL^2)(H_2O)Cl_2].2H_2O$	50 - 150 155- 380 380 – 560 560 - 940	95 305 465 630, 670	1 1 1 2	3.10 (4.77) 19.92 (19.36) 35.48 (35.01) 29.08 (28.38)	87.76 (87.52)	Loss of $2H_2O$. Loss of H_2O and $C_3H_7Cl_2N$. Loss of $C_8H_8Br_2$. Loss of $C_{12}H_{10}N_2O$.	CdO
$[Sn(HL^2)(H_2O)_3].Cl_2$	50 - 330 330 - 625 625 – 1000	245 420 825, 865	1 1 2	22.23 (22.54) 20.68 (20.92) 39.56 (38.91)	82.47 (82.37)	Loss of $3H_2O$ and $C_2H_8Cl_2N$. Loss of C_5H_5BrN. Loss of $C_{16}H_{10}BrN$.	SnO

n* = number of decomposition steps

IJASRM International Journal of Advanced Scientific Research and Management, Vol. 2 Issue 8, August 2017.
www.ijasrm.com
ISSN 2455-6378

4.8 Structural interpretation

The structures of the synthetized metal complexes of H_2L^1 and HL^2 ligands Fe(III), Co(II), Cd(II) and Sn(II) were characterized by elemental analyses, molar conductance, magnetic and thermal analysis techniques. From the elemental analysis, it was established that the two ligands and their complexes were soluble in ethanol and the complexes formed by 1:1 ratio. From IR and ^1H NMR spectra, it could be concluded that H_2L^1 ligand behaved as amono-negative tridentate ligand while HL^2 ligand acted as neutral tridentate ligand. From the molar conductance data, it was found that both the two Sn(II) complexes have an electrolyte nature while the Cd(II) complexes are not electrolytes. Finally the octahedral structure of the complexes was proved from the electronic spectral data.

4.9 Biological activity

The prepared Cd(II) and Sn(II) metal complexes have higher antibacterial activity than that of the free ligands which can be related to the chelation of the Schiff base with metal ions [17] as metal chelates displaying both polar and nonpolar properties; this creates a proper molecules for the penetration into cells and tissues. The polarity of the metal ion will be reduced to a greater extent because of the overlap of the ligand orbital upon chelation process, and partial sharing of the positive charge of the metal ion with donor groups [18,19]. Chelation enriches the delocalization of π-electrons over the whole chelating ring and prompts the penetration of the complexes into lipid membranes [10,17]. It also increases the lipophilic and hydrophilic nature of the central metal ions contributing in liposolubility and permeability through the lipid layer of cell membranes. As well as, lipophilicity, which accountable for the molecules entry rate into the cell, is enhanced by coordination, so the metal complex can become more active than the free Schiff base ligands [10].

Schiff base ligands and their complexes were screened for antibacterial and fungicidal activities. The results was recorded in Table (4) and Figure (4) showed that complexes displayed more inhibitory effects than the parent ligand.

Antibacterial activity was tested in vitro against *Streptococcus aureus*; *Bacillus Subtilis*; *Salmonella SP*. and *Escherichia coli*.

The antibacterial studies showed that, by using *Streptococcus aureus* as Gram-positive bacteria, the HL^2 and the metal complexes recorded their biological activity while H_2L^1 ligand didn't show any activity toward it.

Using *Bacillus Subtilis* as Gram-positive bacteria, the both the two ligands and $[Cd(HL^1)(H_2O)_2Cl].2H_2O$ complex didn't have any biological activity towards it, on the other hand, $[Sn(HL^1)(H_2O)_3]Cl.3H_2O$, $[Cd(HL^2)(H_2O)Cl_2].2H_2O$ and $[Sn(HL^2)(H_2O)_3].Cl_2$ complexes showed a biological activity but $[Cd(HL^2)(H_2O)Cl_2].2H_2O$ complex was the highest of them.

Using *Salmonella SP*. as Gram-negative bacteria, $[Sn(HL^2)(H_2O)_3].Cl_2$ complex has the highest biological activity of all of them.

Using *Escherichia coli* as Gram-negative bacteria, all of them recorded their biological activity towards it as mentioned in Table (4).

For fungicidal activity, compounds were screened in vitro against *Aspergillus fumigatus* and *Candida albicans*.

The antifungal studies showed, by using *Candida albicans*, $[Cd(HL^1)(H_2O)_2Cl].2H_2O$ complex showed the highest biological activity while $[Sn(HL^1)(H_2O)_3]Cl.3H_2O$ complex didn't record any activity.

Using *Aspergillus fumigatus*, the highest biological activity was that of the $Cd(HL^1)(H_2O)_2Cl].2H_2O$ complex and the lowest activity was that of the $[Sn(HL^1)(H_2O)_3]Cl.3H_2O$ complex. While there wasn't any biological activity for the H_2L^1 ligand and $[Sn(HL^2)(H_2O)_3].Cl_2$complex.

The activities of the formed Schiff base ligand and its metal complexes were proved by calculating the activity index according to the following relation and that showed in Figure (2) [17,20]:

Activity index (A) = [Inhibition Zone of compound (mm) / Inhibition Zone of standard drug (mm)] ×100

From the previous data, it is concluded that Cd(II) complexes had the highest activity index in most cases.

IJASRM
International Journal of Advanced Scientific Research and Management, Vol. 2 Issue 8, August 2017.
www.ijasrm.com
ISSN 2455-6378

Table (4). Biological activity of H_2L^1, HL^2 ligand and their Cd(II) and Sn(II) metal complexes.

Sample		Inhibition zone diameter (mm / mg sample)					
		Gram positive bacteria		Gram negative bacteria		Fungus	
		Staphyococcus aureus	***Bacillus subtilis***	***Salmonella SP.***	***Escherichia coli***	***Aspergillus fumigates***	***Candida alibicans***
$[H_2L^1]$		NA	NA	10	14	11	NA
$[Cd(HL^1)(H_2O)_2Cl].2H_2O$		10	NA	12	14	13	15
$[Sn(HL^1)(H_2O)_3]Cl.3H_2O$		12	9	12	12	NA	10
$[HL^2]$		12	NA	13	12	12	11
$[Cd(HL^2)(H_2O)Cl_2].2H_2O$		12	12	13	14	12	14
$[Sn(HL^2)(H_2O)_3].Cl_2$		12	10	14	12	10	NA
Standard	Amikan	9	6	7	6	---	---
	Ketokonazole	---	---	---	---	9	9

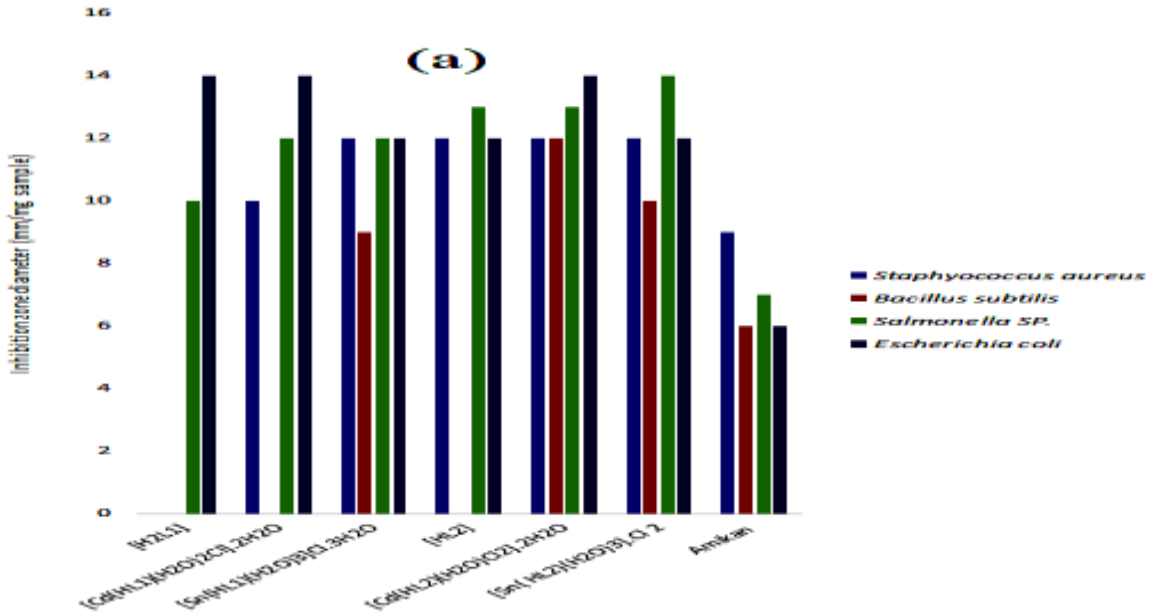

IJASRM
International Journal of Advanced Scientific Research and Management, Vol. 2 Issue 8, August 2017.
www.ijasrm.com
ISSN 2455-6378

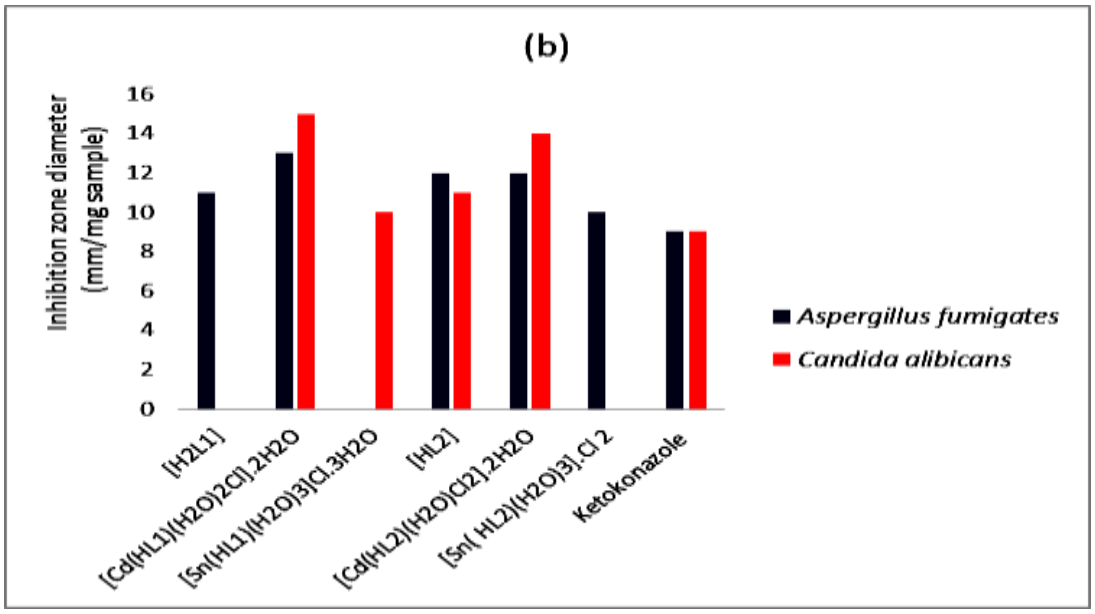

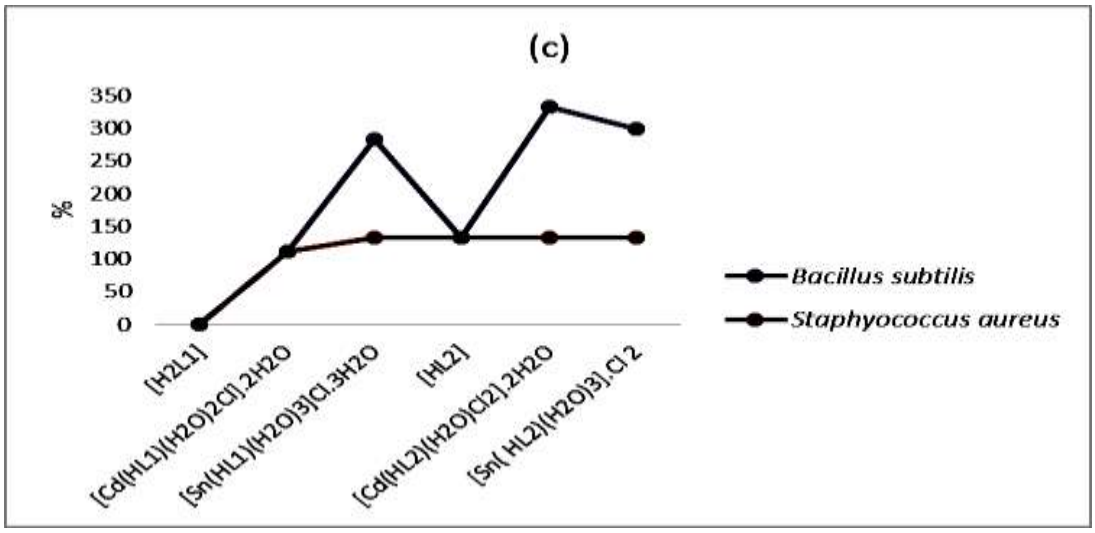

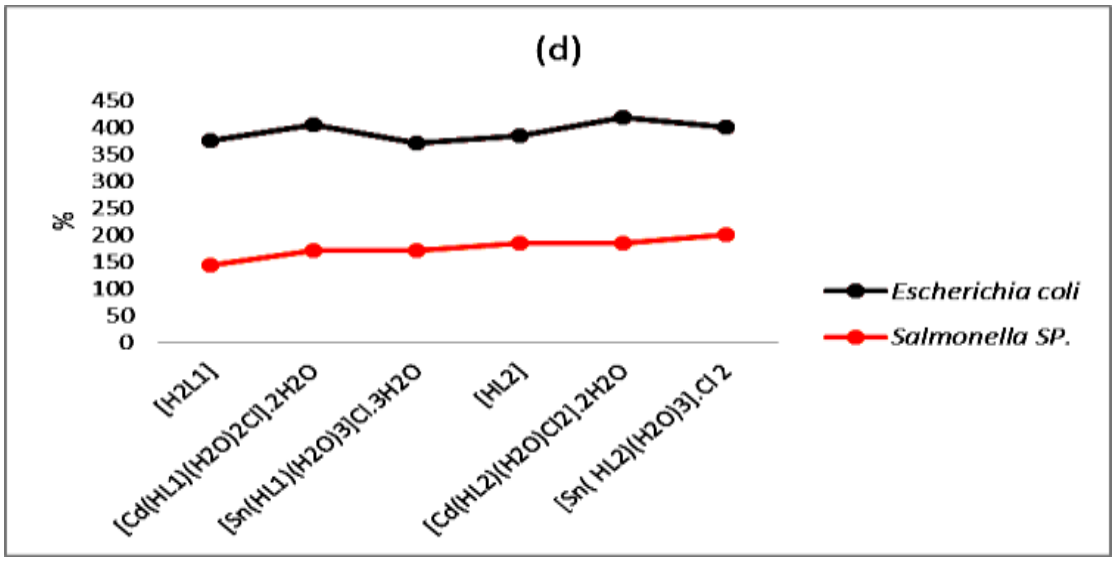

IJASRM
International Journal of Advanced Scientific Research and Management, Vol. 2 Issue 8, August 2017.
www.ijasrm.com
ISSN 2455-6378

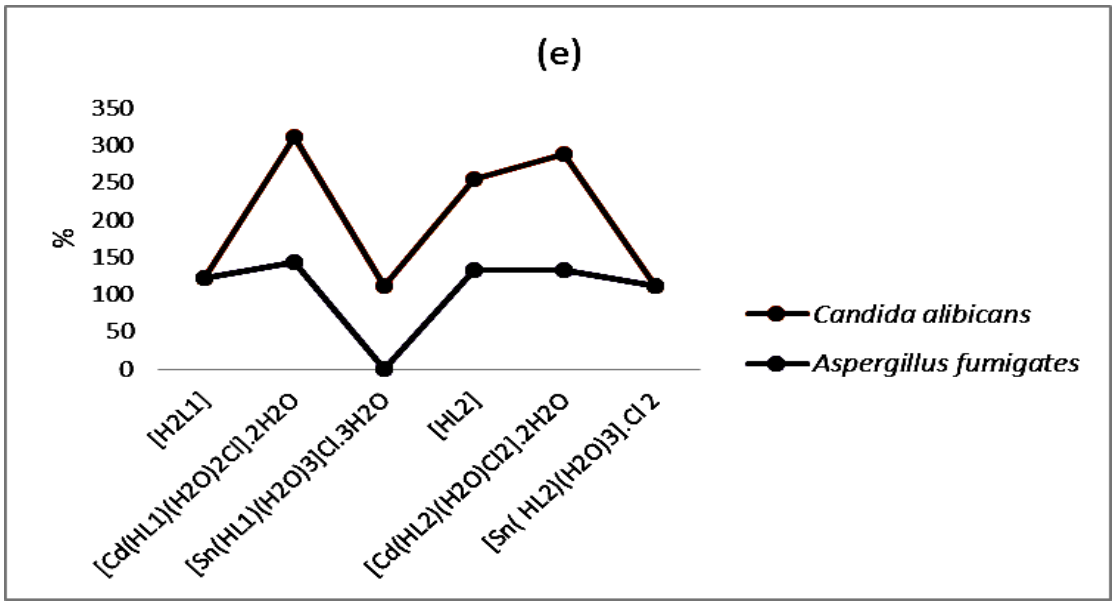

Figure 4. Biological activity of the two Schiff base ligands and their metal complexes against (a) different bacterial species (b) different fugal species and (c, d and f) Activity index values.

5. Summary and Conclusion

Novel Schiff base H_2L^1 and HL^2 ligands were synthesized as the condensation product subsequent from the reaction between 2-hydroxybenzaldehyde and 2-quinoline carbaldehydev with ambroxol drug, respectively. Cd(II) and Sn(II) metal were coordinated with the Schiff base ligands, where all the resulting complexes evidenced to be of the MHL type and were formed by 1:1 ratio of metal salt: ligand, as confirmed by the elemental analysis. Both of the IR and ^{1}H NMR spectra have indeed confirmed that the H_2L ligand behaves as a mono-negative tridentate ligand that coordinates to the metal ions via two nitrogen atoms (the azomethine nitrogen as well as the amino nitrogen) and one oxygen atom of deprotonated phenolic group while HL^2 ligand acts as a neutral tridentate ligand that binds to the metal ion through three nitrogen atoms (azomethine nitrogen, ambroxol nitrogen and the pyridine nitrogen). The expected general formula of the formed complexes is $[M(HL)(H_2O)_xCl_y]Cl_n.(H_2O)_m$. Cd(II) complexes are determined as non-electrolytes, as shown by conducti-metric measurements. On the other hand, the molar conductance of $[Sn(HL^1)(H_2O)_3]Cl.3H_2O$ complex confirmed its ionic nature and that they are of type 1:1 electrolytes, while the stoichiometry of the $[Sn(HL^2)(H_2O)_3].Cl_2$ complex is 1:2 as shown by its molar conductance value. All the complexes exhibited octahedral geometry that is confirmed by the electronic transition spectra. The antimicrobial activity test proved that Cd(II) complex had the highest activity index. Therefore, the results of this present study will hopefully facilitate the research for the synthesis and application of novel metal complexes based on the newly prepared Schiff base (H_2L).

6. Acknowledgment

The authors gratefully acknowledge the support of Nile Pharma for providing the ambroxol drug.

References

[1] Ahmed M. Abu-Dief and Ibrahim M.A. Mohamed, "A review on versatile applications of transition metal complexes incorporating Schiff bases," *Beni-Suef University Journal of Basic and Applied Sciences*, vol. 4, pp. 119-133, 2015.

[2] Abdur Rauf et al, "Synthesis, spectroscopic characterization, DFT optimization and biological activities of Schiff bases and their metal (II) complexes," *Journal of Molecular Structure*, vol. 1145, pp. 132-140, 2017.

[3] Anant Prakash and Devjani Adhikari, "Application of Schiff bases and their metal complexes-A Review," *International Journal of ChemTech Research*, vol. 3, pp. 1891-1896, 2011.

[4] Rajesh, P. et al, "Structural, spectral analysis of ambroxol using DFT methods," *J. of Molecular Structure*, vol. 1144, pp. 379-388,

2017.

[5] Pfaller M.A. et al, "Multicenter evaluation of a broth macrodilution antifungal susceptibility test for yeasts," *J. Clin. Microbiol.*, vol. 26, pp. 1437-1441, 1988.

[6] *National Committee for Clinical Laboratory Standards. Reference method for broth dilution antifungal susceptibilty testing of conidium-forming filamentous: proposed standard M38-A. Wayne, PA, USA*, 2002.

[7] *National Committee for Clinical Laboratory Standards. Method for antifungal disc diffusion susceptibility testing of yeast: proposed guideline M44-P, Wayne, PA, USA*, 2003.

[8] Mahmoud W.H. et al, "“Synthesis , Characterization and in vitro Biological Activity of Mixed Transition Metal Complexes of Lornoxicam with 1,10-phenanthroline” ," *Spectrochim.Acta A. J. Mol. Biomol.Spectrosc.*, vol. 122, pp. 598-608, 2014.

[9] Sakıyan I. et al, "Antimicrobial activities of N-(2-hydroxy-1-naphthalidene)-amino acid(glycine, alanine, phenylalanine, histidine, tryptophane) Schiff bases and their manganese(III) complexes.," *BioMetals*, vol. 17, pp. 115-120, 2004.

[10] Mahmoud W.H. et al, "Novel Schiff base ligand and its metal complexes with some transition elements. Synthesis, spectroscopic, thermal analysis, antimicrobial and in vitro anticancer activity. Appl. Organometal.," *Appl. Organometal. Chem.*, vol. 30, pp. 221-230, 2016.

[11] Linert A.A. and Abou-Hussein W., "Synthesis, spectroscopic studies and inhibitory activity against bactria and fungi of acyclic and macrocyclic transition metal complexes containing a triamine coumarine Schiff base ligand," *Spectrochim. Acta A* , vol. 141, pp. 223-232, 2015.

[12] Abo-Aly M.M. et al, "Spectroscopic and structural studies of the Schiff base 3-methoxy-N-salicylidene-o-amino phenol complexes with some transition metal ions and their antibacterial, antifungal activities," *Spectrochim. Acta A*, vol. 136, pp. 993-1000, 2015.

[13] Shafaatian B. et al, "Synthesis, characterization, single crystal X-ray determination, fluorescence and electrochemical studies of new dinuclear nickel(II) and oxovanadium(IV) complexes containing double Schiff base ligands," *Spectrochim. Acta A*, vol. 5, pp. 248-255, 2014.

[14] El-Sonbati A.Z. et al, "Molecular docking, DNA binding, thermal studies and antimicrobial activities of Schiff base complexes," *Journal of Molecular Liquids*, vol. 218, pp. 434-456, 2016.

[15] Mahmoud W.H. et al, "New bioactive Pt(II) binary and ternary metal complexes with guaifenesin drug: Synthesis, geometrical structure, and spectroscopic and thermal characterization," *Appl. Organometal. Chem.*, vol. Accepted manuscripit, 2016.

[16] Kumar G. et al, "Synthesis of Schiff base 24-membered trivalent transition metal derivatives with their anti-inflammation and antimicrobial evaluation," *Journal of Molecular Structure.*, vol. 1108, pp. 680-688, 2016.

[17] Joseyphus R.S. and Nair M.S., "Antibacterial and Antifungal Studies on Some Schiff Base Complexes of Zn(II)," *J. Mycrobiology*, vol. 36, pp. 93-98, 2008.

[18] Siji V.L. et al, ""Synthesis, Spectroscopic Characterization, and Antimicrobial Activity of Cobalt(II) Complexes of Acetone-N(4) Phenylsemicar- bazone: Crystal Structure of [Co(HL)2(MeOH)2](NO3)2" ," *Transition Metal Chemistry*, vol. 36, pp. 417-424, 2011.

[19] Tu¨rkkan B. et al, ""Synthesis, Characterization and Antimicrobial Activity of 3,5-Di- Tert-Butylsalicylaldehyde-S-Methylthiosemicarbazones and Their Ni(II) Complexes" ," *Transition Metal Chemistry*, vol. 36, pp. 679-682, 2011.

[20] Mohammad Habib et al, "Synthesis, experimental and theoretical characterizations of a new Schiff base derived from 2-pyridincarboxaldehyde and its Ni (II) complex," *J. of Molecular Structure*, vol. 1143, pp. 424-430, 2017.